

Article

Development and Application of Similar Materials for Foundation Pit Excavation Model Test of Metro Station

Zeyao Zhang ^{1,2}, Yang Gao ^{1,2,*}, Xinyu Zheng ^{1,3}, Jiarui Cao ² and Yong Chen ²

¹ School of Safety Engineering and Emergency Management, Shijiazhuang Tiedao University, Shijiazhuang 050043, China

² Key Laboratory of Large Structure Health Monitoring and Control, Shijiazhuang Tiedao University, Shijiazhuang 050043, China

³ Geotechnical and Structural Engineering Research Center, Shandong University, Jinan 250061, China

* Correspondence: gaoyang_sjz@163.com

Abstract: Geomechanical model tests provide an intuitive and convenient method for observing physical phenomenon due to their easy implementation compared to in situ tests and prototype tests. The success of model tests depends heavily on the appropriate selection of model materials and proportions. Therefore, a new similar material is developed by utilizing the orthogonal experimental design method to conduct a series of proportioning tests. The new material is mixed with barite powder, iron ore powder, quartz sand, liquid paraffin, rosin, gypsum powder, and water. The physical and mechanical properties are studied through uniaxial compressive tests, Brazilian splitting tests, and direct shear tests. The influences of various raw material factors on the parameters of the similar material are systematically studied through range analysis. The results demonstrate that the mechanical parameters of similar materials have wide variation ranges; the adjustment range is 42.0–279.0 MPa for the elastic modulus, 0.37–5.37 MPa for the uniaxial compressive strength and 2.23–2.65 g/cm³ for the density. The new similar material has illustrated advantages in terms of performance stability, low price, and convenient production, which can simulate the similar relationship with different geomechanical model tests. The similar material is applied to a 3D geomechanical model test of the foundation pit excavation of Shenzhen metro station, which proves that the similar material can realistically reflect the change of earth pressure in the excavation process. With the deepening of excavation, the earth pressure curve shows significant fluctuations, and as the retaining structure is displaced, the parts with large earth pressure changes should be strengthened. The research methods and results can provide reference for further geological engineering research.

Keywords: foundation pit excavation; mechanical properties; orthogonal experiment; range analysis; geomechanical model test



Citation: Zhang, Z.; Gao, Y.; Zheng, X.; Cao, J.; Chen, Y. Development and Application of Similar Materials for Foundation Pit Excavation Model Test of Metro Station. *Appl. Sci.* **2022**, *12*, 12880. <https://doi.org/10.3390/app122412880>

Academic Editor: Ana Paula Betencourt Martins Amaro

Received: 10 November 2022

Accepted: 12 December 2022

Published: 15 December 2022

Publisher's Note: MDPI stays neutral with regard to jurisdictional claims in published maps and institutional affiliations.



Copyright: © 2022 by the authors. Licensee MDPI, Basel, Switzerland. This article is an open access article distributed under the terms and conditions of the Creative Commons Attribution (CC BY) license (<https://creativecommons.org/licenses/by/4.0/>).

1. Introduction

Urban developments have raised challenges such as land shortages and traffic congestion which have become increasingly prominent with the growth of cities [1]. The development and utilization of underground space can help alleviate issues caused by urbanization [2]. However, in some complex and crowded environments, the excavation of foundation pits affects the stress state of soil in adjacent areas [3,4], which will lead to strength failure, deformation, and instability. At present, methods for excavation stability research mainly consist of on-site monitoring, theoretical research, numerical simulation, and model tests [5–9]. For some intricate large-scale projects, on-site monitoring imposes difficulty with controlling variables and cannot explore the state of stress changes within the rock mass structure [10–12]. Though theoretical research and numerical simulation have been widely utilized to describe the excavation of foundation pits, they still have limitations under complicated working conditions and face difficulties in recreating the real site's mechanical state. As a result, model tests become an indispensable method. Geomechanical model tests

using similar materials can effectively simulate the complete process of structural stress in complex environments in addition to more intuitively revealing earth pressure characteristics and deformation [13]. Zhang [14] studied the mechanical properties of a subway station retaining structure adjacent to the pile foundation by using laboratory the model testing method. Wang [15] developed a centrifugal model test of a power plant excavation project in order to reveal the interaction mechanism between piles and soils during foundation pit excavation. On the other hand, however, these model tests only reduced the size without giving consideration to the scale change of material mechanical parameters. In combination with the similarity theory, it is known that test materials must maintain an appropriate scale ratio with the prototype medium. Therefore, the selection of an appropriate similar material is the guarantee for successful geomechanical model tests [16,17].

It is of great significance to study the influence of material components and proportions on the mechanical properties of a similar material [18]. Scholars have researched similar materials for model tests in the past. In the 1960s, two institutes, ISMES in Italy and LNEC in Portugal, successively proposed model materials for geomechanics engineering model tests [19,20]. The MIB material developed by Han et al. [21] is a similar material made by stirring and mixing iron ore powder, barite powder, rosin alcohol solution, and membraniferous iron powder. However, this material produces toxic substances during the filming of iron ore powder. Ma et al. [22] developed a geomechanical model material (NIOS), which is characterized as non-toxic, heavy, low-price, and of stable performance. However, the model dries slowly and the curing time is long. Zhu et al. [23,24] combined the advantages of MIB and NIOS to develop a similar material which is more suitable for the geomechanics model tests of geotechnical engineering, and applied it to boundary loading model tests. Zhang et al. [25] systematically analyzed the principle of similar material combinations and proposed a new similar material which can simulate different rock masses. At present, some achievements have been made in the relevant studies, but there is still a lack of systematic development of similar materials for foundation pit excavation model tests.

In summary, in order to accurately simulate the mechanical evolution process during the excavation of a foundation pit structure, it is urgent to develop a new type of similar material that satisfies the similarity conditions of model tests. In comparisons with existing research [26–28], this study makes full use of the brittleness of rosin and the plasticity of liquid paraffin, and a new type of similar material with large adjustable characteristic is proposed for which barite powder, iron ore powder, and quartz sand are selected as aggregates, gypsum powder is used as a regulator, and non-water-soluble liquid paraffin and rosin are selected as cementing agents. Based on the orthogonal experimental method [29,30], mechanical parameter tests of different proportioning materials are performed. Subsequently, the effect of each raw material on the parameters of the similar material is studied by range analysis. Finally, in accordance with the above research, a further physical model test based on the excavation of metro stations is conducted using the new similar material, revealing that the earth pressure changes in limited spaces with soil masses of different aspect ratios. In conclusion, this research can provide a reference for the mechanical evolution law of practical metro station excavation and construction.

2. Similarity Principle

Based on the principle of similitude, the test model and the prototype must have the same physical quantities and be able to be expressed by the same relationship. Therefore, all physical parameters with the same dimension should maintain the same constant ratio [31,32]. The similarity scale C is defined as the ratio of physical quantities with the same dimension between the prototype and model [33]. The geomechanical model test requires that the similarity ratios of dimensionless quantities are 1 and that the similarity ratio of the same dimensional physical quantities is equal. According to displacement

boundary conditions, stress boundary conditions, and physical equations, the parameters of materials for model tests should satisfy the following similar relationships [34,35].

$$C_\varepsilon = C_f = C_\varphi = C_\mu = 1 \quad (1)$$

$$C_\sigma = C_E = C_c = C_{\sigma_c} = C_{\sigma_t} \quad (2)$$

where C_ε , C_f , C_φ , C_μ , C_σ , C_E , C_c , C_{σ_c} and C_{σ_t} represent the similarity ratio of the strain, friction coefficient, internal friction angle, Poisson's ratio, stress, elastic modulus, cohesive force, compressive strength, and tensile strength, respectively.

The similar relationship among stress similarity ratio, bulk density similarity ratio, and geometric similarity ratio is given as follows:

$$C_\sigma = C_\gamma C_L \quad (3)$$

The similar relationship among displacement similarity ratio, strain similarity ratio, and geometric similarity ratio is given as follows:

$$C_\delta = C_\varepsilon C_L \quad (4)$$

The similar relationship among stress similarity ratio, strain similarity ratio, and elastic modulus similarity ratio is given as follows:

$$C_\sigma = C_\varepsilon C_E \quad (5)$$

3. Development of Similar Materials

3.1. Selection of Similar Materials

Developing similar materials for geomechanical model tests should satisfy the main requirements of five aspects: (1) the key physical and mechanical parameters should have certainly similarity to real soil mass. (2) Similar materials consist of granular materials. The dense structure and large friction angle can be guaranteed through compressing into a certain size of block in the model. (3) The key physical parameters of the similar material can be widely adjusted by changing the materials' ratio to apply to different working conditions. (4) The molded materials have high electrical insulation and stability and are not affected by changes in temperature and humidity. (5) The manufacturing process of the similar materials is convenient and nontoxic.

In accordance with the multiple requirements of the similar material for mechanical parameters, combined with the advantages of the IBSCM material, iron ore powder, barite powder, and quartz sand were selected as aggregates, and gypsum powder was utilized as a regulator. In comparison with the IBSCM material [36], liquid paraffin was used instead of alcohol, and rosin was used as a cementing agent, as it dissolves slowly in alcohol with a high concentration. After reaching the saturation level, rosin will not dissolve. In addition, rosin is brittle, while liquid paraffin has the characteristic of plasticity. Therefore, the mixture of the two can be applied as a cementing agent in order to enlarge the adjustment range of the physical parameters of the model material. The compositions of the similar material are shown in Figure 1.

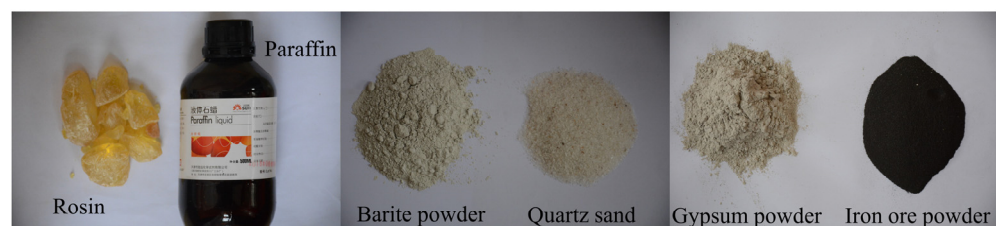


Figure 1. Main compositions of the similar material.

3.2. Design Scheme of Orthogonal Test

According to the requirements of the model tests of metro excavation on the physical parameters of the similar material, the orthogonal experimental design method is utilized to reveal the effects of different factors on the mechanical parameters of the new similar material. In order to meet the functional requirements of the material, 80 mesh iron ore powder, 200 mesh barite powder, and 3 types of quartz sand—10–20 mesh, 20–40 mesh, and 40–80 mesh—were selected to adjust the properties of the mixed material through different gradations.

In this orthogonal experimental design, four factors were set up, namely A: the iron ore powder and barite powder content; B: the cementing agent content; C: the molar concentration of the cementing agent; and D: the mesh number of the quartz sand. Other parameters included the proportion of barite powder and iron ore powder being 7:3 and gypsum accounting for 1.5% of the total mass. As demonstrated in the test configuration experience, three levels were set for each factor, and the selected parameters are shown in Table 1. According to the four factors and three levels determined by the orthogonal test, the orthogonal table L₉ (3⁴) was selected, which means that nine sets of tests were carried out. The material orthogonal test scheme is shown in Table 2.

Table 1. Orthogonal design of the similar material.

Level	Factor			
	A	B	C	D
1	65	3	20	10–20
2	75	6	40	20–40
3	85	9	60	40–80

Table 2. Orthogonal test scheme of the material.

Level	Factor			
	A	B	C	D
1	65	3	20	10–20
2	65	6	40	20–40
3	65	9	60	40–80
4	75	3	40	40–80
5	75	6	60	10–20
6	75	9	20	20–40
7	85	3	60	20–40
8	85	6	20	40–80
9	85	9	40	10–20

3.3. Preparation of Specimens

To study the effects of different factors on the mechanical parameters of the material, standard specimens of the model materials were made following the proportions for an orthogonal test. A steel mold with height of 100 mm and a diameter of 50 mm was utilized to make standard specimens for investigating the mechanical parameters of the similar material with different proportions. As shown in Figure 2, the process of producing the standard specimens was as follows. First, the quartz sand, barite powder, iron ore powder, and gypsum powder were weighed as consistent with the proportion, and the mixture was stirred evenly. Next, the paraffin and rosin were heated up until they were in liquid state, after which this liquid was immediately added to the mixture, and it was further gently mixed to a uniform state. When the mixture was ready, and it was poured into the mold and fully vibrated with compaction. Finally, after disassembling the mold and marking the standard specimens, they were cured at room temperature for 2–3 days.



Figure 2. Similar material specimens-making process.

3.4. Mechanical Parameters Testing of Similar Materials

Uniaxial compressive strength test, Brazilian splitting test, and direct shear test were carried out on the standard specimens. A total of 125 groups of tests were conducted, for which each group consisted of 4 to 6 specimens. A uniaxial compression test was performed on the test machine, as shown in Figure 3, during which the uniaxial compressive strength was measured for specimens with $\varphi 50 \text{ mm} \times 100 \text{ mm}$, and the complete stress–strain curve was obtained. A Brazilian splitting test was conducted on specimens with $\varphi 50 \text{ mm} \times 50 \text{ mm}$ in order to determine the tensile strength.

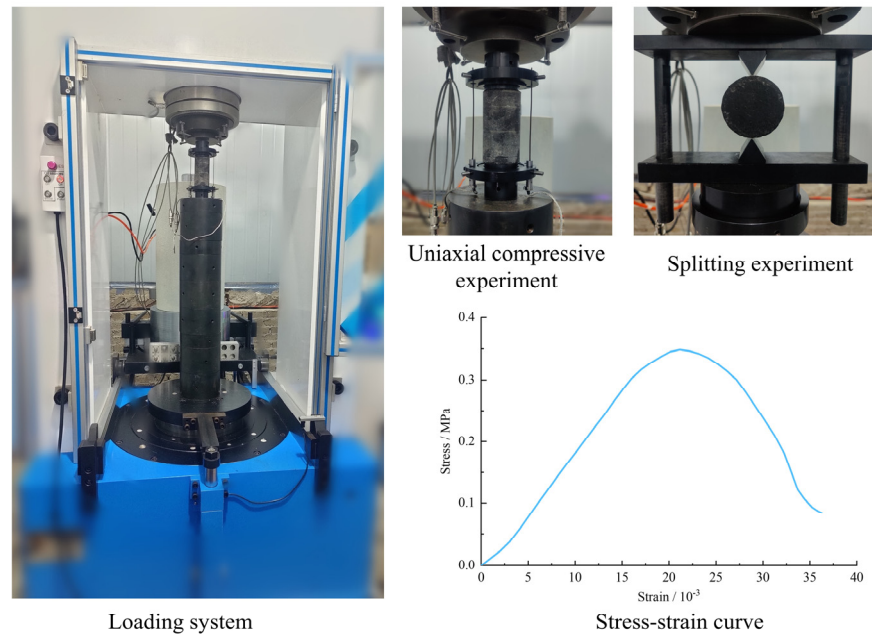


Figure 3. Uniaxial compression test of the material.

A direct shear test was carried out on a SDJ-1 strain controlled direct shear apparatus, as shown in Figure 4, by which the cohesion and internal friction angles of similar materials with different mixing ratios were measured. The shear strength was calculated as shown in Equation (6):

$$\tau = \sigma \tan \theta + c \tag{6}$$

where σ is normal stress and τ is shear strength. By applying different normal stress σ , the corresponding shear strength τ can be obtained. The least square method was used to fit the data in order to obtain the values of cohesion c and internal friction angle φ .

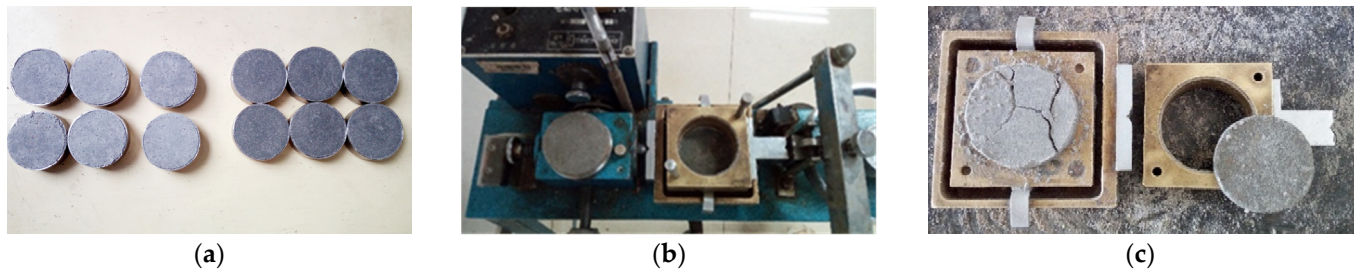


Figure 4. Direct shear test. (a) Direct shear specimens. (b) Direct shearing apparatus. (c) Specimens' failure state.

4. Range Analysis

By conducting nine sets of orthogonal tests with various proportions, the physical and mechanical parameters were measured for material specimens with different proportions, including density ρ (g/cm^3), compressive strength σ_c , tensile strength σ_t , cohesion C , elastic modulus E , and friction angle φ . Table 3 shows the test results, and the density of the similar material is 2.23–2.65 g/cm^3 . The similar material has a higher bulk density, which is consistent with the actual cohesionless soil bulk density on site. Therefore, it can simplify the conversion of physical parameters between the model and the prototype. On the other hand, the tensile–compression ratio of the similar material is 1/8.5–1/11.7, indicating that the similar material can better simulate the tensile properties of the prototype. Furthermore, the compressive strength ranges from 0.37 to 5.37 MPa, the elastic modulus ranges from 42.0 to 279.0 MPa, the cohesion ranges from 42.7 to 57.3 kPa, and the friction angle ranges from 28.37° to 37.04°. The above experiment results demonstrate that these mechanical parameters have a large variation range which can meet the requirements of the various mechanical parameters of the similar material in different testing conditions.

Table 3. Summary of test results.

Test	ρ (g/cm^3)	σ_c (MPa)	σ_t (MPa)	E (MPa)	C (kPa)	φ (°)
1	2.46	0.69	0.071	248.67	46.359	37.04
2	2.47	3.47	0.363	237.33	50.904	30.73
3	2.33	1.10	0.097	96.33	51.813	28.37
4	2.23	2.24	0.211	256.00	57.267	31.12
5	2.46	5.37	0.498	279.00	42.723	29.72
6	2.53	0.34	0.029	50.67	46.359	29.80
7	2.39	2.02	0.235	217.33	55.449	28.77
8	2.46	0.62	0.058	157.33	46.359	30.96
9	2.65	0.37	0.033	42.00	45.450	28.61

This paper adopts range analysis to study the results. Generally, X_{ij} is defined as the value of the i -th level of factor j ($i = 1, 2, \dots, n, j = A, B, C, D$). Experiments under X_{ij} are conducted in order to obtain the result index Y_{ij} of the i -th level of factor j , where Y_{ij} are random variables that follow the normal distribution. Conducting P_1 tests under X_{ij} can produce P_1 test results ($Y_{ijk} = 1, 2, \dots, P_1$). In Formula (7), K_{ij} is the statistical parameter of the j -th factor at the i -th level, while Y_{ijk} is the index value of the k -th test result of the j -th factor at the i -th level.

$$K_{ij} = \sum_{k=1}^{P_1} Y_{ijk} \quad (7)$$

The range refers to the difference between the extreme values of the data, which reflects the degree of dispersion of the data. The larger the range, the more sensitive the factor [36].

The factors with the largest range would be the most significant. Generally, the five main parameters of density, compressive strength, elastic modulus, cohesion, and friction angle can effectively control the physical and mechanical characteristics of materials. Therefore, these five parameters are utilized to carry out range analysis and determine the order of effect of the factors. The range analysis results of influencing factors are shown in Table 4.

Table 4. Summary of range analysis results.

Parameter	Level	Factor			
		A	B	C	D
ρ (g/cm ³)	1	2.42	2.30	2.48	2.52
	2	2.41	2.46	2.45	2.46
	3	2.50	2.50	2.39	2.34
	Range	0.09	0.14	0.09	0.18
σ_c (MPa)	1	1.75	1.65	0.55	2.14
	2	2.65	3.15	2.03	1.94
	3	1.01	0.60	2.83	1.32
	Range	1.64	2.55	2.28	0.82
E (MPa)	1	194.11	240.67	152.22	189.89
	2	195.22	224.56	178.44	168.44
	3	138.89	63.00	197.56	169.89
	Range	56.33	177.67	45.33	21.44
C (kPa)	1	49.69	53.03	46.36	44.84
	2	48.78	46.66	51.21	50.90
	3	49.09	47.87	50.00	51.81
	Range	0.91	6.36	4.85	6.97
φ (°)	1	32.04	32.31	32.60	31.79
	2	30.21	30.47	30.15	29.77
	3	29.45	28.92	28.95	30.15
	Range	2.60	3.38	3.65	2.02

In order to more intuitively investigate the effect of each factor on the five parameters, a diagram of the relationships among the levels of each factor and parameter was produced, and this is shown in Figure 5. The results show that the four factors have certain effects on the mechanical properties of similar materials.

In terms of the densities of specimens, the range of D is greater than those of A, B, and C. The range of factor D is the largest, slightly larger than factor B. Factor D mainly controls the density of the similar materials, and factor B also has a significant effect. As shown in Figure 5a, the density decreases as factors C and D increase, but it increases as factor B increases. In terms of the compressive strengths of specimens, the range of values of factor B is the largest, indicating that B is the most important factor influencing compressive strength. As shown in Figure 5b, the compressive strength first increases and then decreases under the influence of factors A and B, and it increases with the increase of factor C. The influence of each factor on the compressive strength ranged from large to small for B, C, A, and D, respectively. In terms of the elastic modulus of specimens, the range of factor B is much larger than other factors and is the main factor affecting the elastic modulus. As is shown in Figure 5c, the elastic modulus decreases significantly as factors A and B increase. The range of factors C and D is small and has little effect on the elastic modulus. The influence of each factor on the elastic modulus ranged from large to small for B, A, C, and D, respectively. In terms of the cohesion of specimens, the range of factor D is the largest, and it is slightly larger than that of factor B. Factor D is an important factor influencing cohesion, and factor B also has a certain effect on cohesion. As is shown in Figure 5d, the cohesion increases as factor D increases. The cohesion first decreases and then increases under the influence of factor B. The range of factor A is small, so the data have good concentration. The influence of each factor on the cohesion ranged from large to

small for D, B, C, and A, respectively. In terms of the friction angle of specimens, the range of values of factor C is the largest, and it is slightly larger than that of factor B. Factor C mainly controls the friction angle of the similar materials, and factor B also has an obvious influence. As shown in Figure 5e, the friction angle decreases as factors A, B, and C increase. The range of factor D is the smallest, and its influence is not significant. The influence of each factor on the friction angle ranged from large to small for C, B, A, and D, respectively.

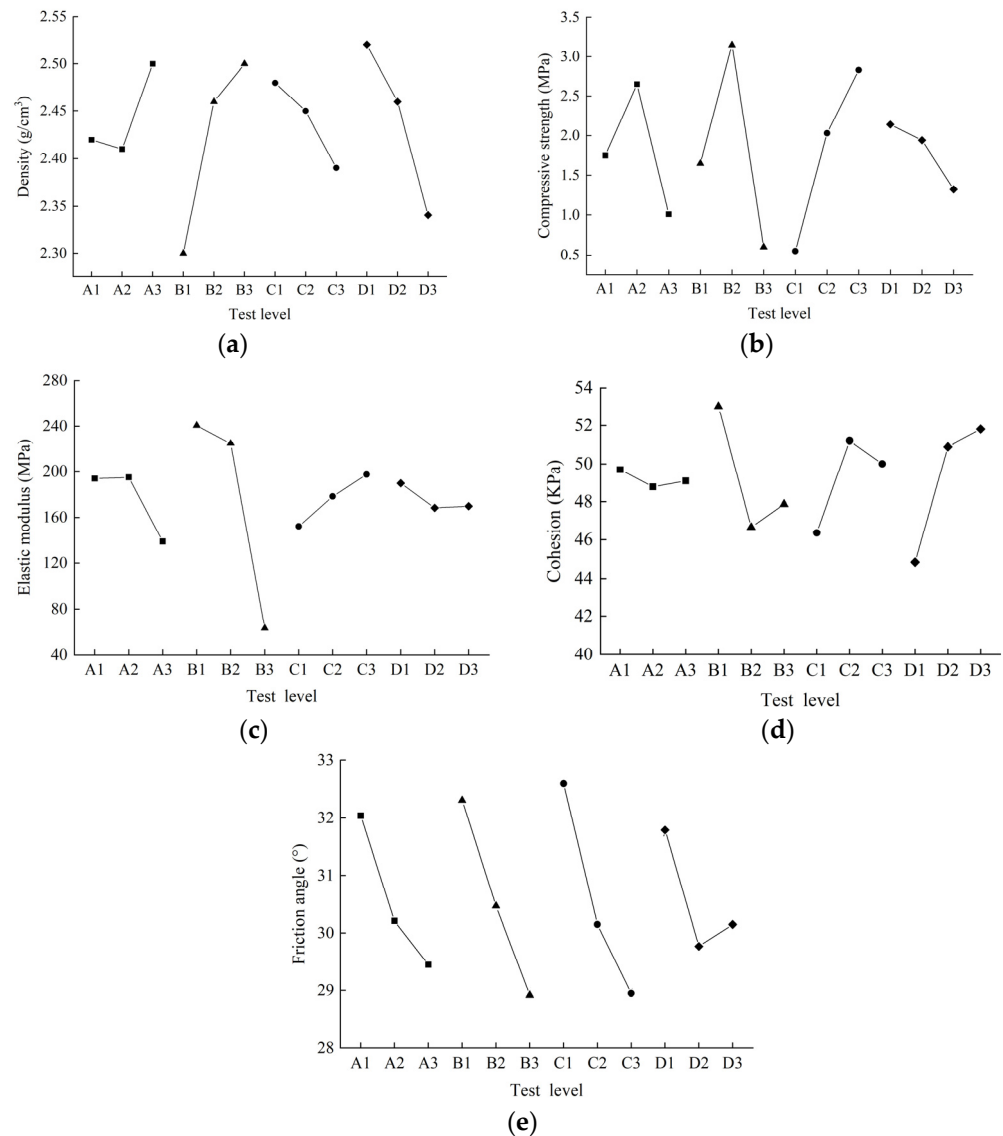


Figure 5. Influencing rule of control factors on mechanical properties of materials: (a) density, (b) compressive strength, (c) elastic modulus, (d) cohesion, and (e) friction angle.

By analyzing the five main parameters, the ranges of compressive strength and elastic modulus corresponding to factor B are 2.55 and 177.67, respectively, which are much larger than the ranges corresponding to the other three factors. On the other hand, the ranges of density, cohesion, and friction angle are also relatively large. Therefore, factor B is the dominating factor affecting the mechanical characteristics of similar materials.

The elastic modulus and compressive strength are the key parameters for analyzing the mechanical properties of materials, which determine deformation law and the ultimate strength of model materials, respectively. The orthogonal test and range analysis proved that cementing agent content has the greatest effect on these two mechanical parameters. Through adjusting the cementing agent content in order to investigate the changing rules of similar materials' compressive strength and elastic modulus under the promise of keeping

other factors unchanged. Figure 6 shows the relationship between the cementing agent content and compressive strength and elastic modulus. With the increase of cementing agent content, the elastic modulus of the material decreases gradually, while the compressive strength first increases and then decreases. The change trend is highly consistent with the results of the range analysis. The use of paraffin as cement has a significant impact on similar materials. Notably, controlling the content of cement within 9% can effectively guarantee the molding of the similar materials.

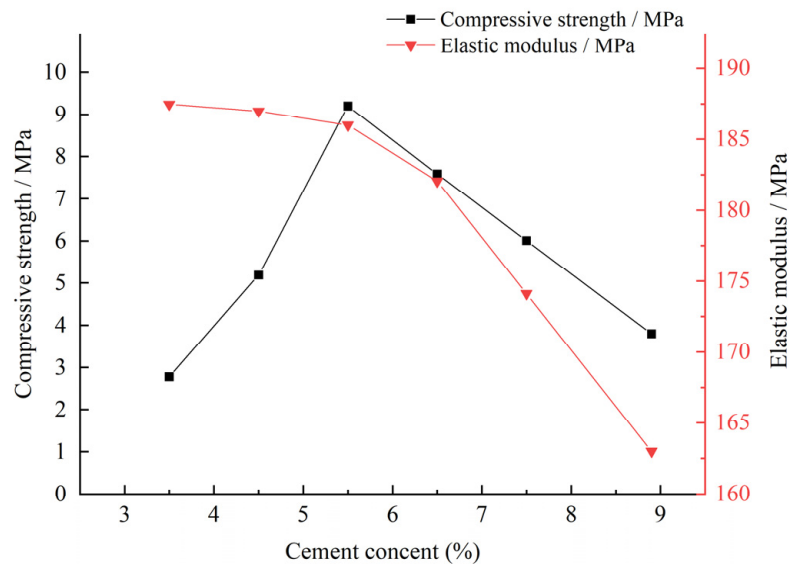


Figure 6. Curves of the compressive strength and elastic modulus at different cementing agent contents.

5. Application of Metro Station Excavation Model Test

5.1. Overview of the Model Test

Chegongmiao Station, a four-line transfer station of Shenzhen metro, is located adjacent to two other underground structures, as show in Figure 7. The existing structures around the metro expansion project are complex. The minimum clear distance between the metro station and the existing building on the east side is only 3.45 m, and the station structure is built in conjunction with the viaduct on the west side; as a results, its foundation pit construction can only be carried out in a narrow environment.

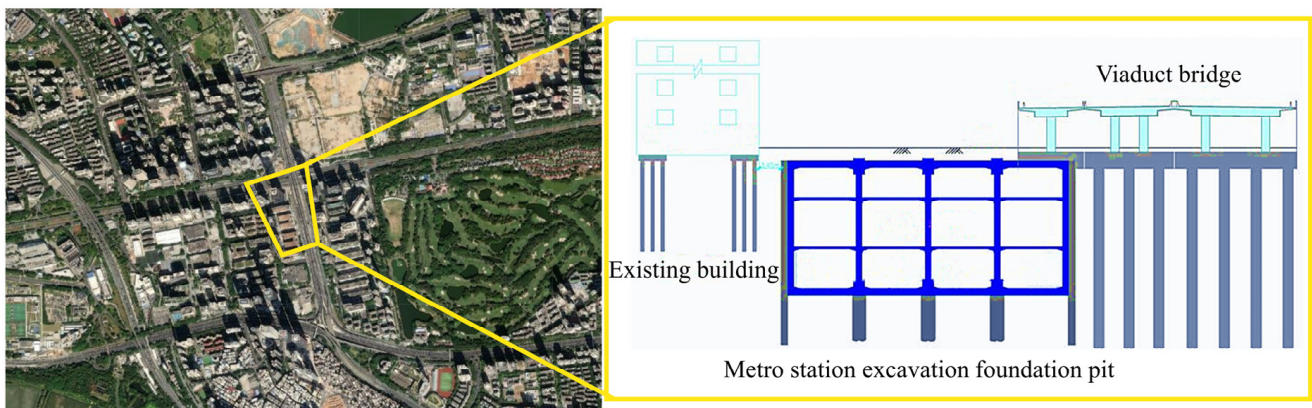


Figure 7. Location site of the metro station foundation pit.

Based on this practical project, a geomechanical model test was carried out to study the earth pressure changing law of the soil mass during the excavation of the long, narrow metro station foundation pit. In this study, the geometry similarity ratio is $C_h = 50$, while the elastic modulus similarity ratio is $C_E = 10$. For ease of conversion, the stress similarity

ratio was taken as $C_\sigma = 50$. The dimensions of the prototype foundation pit were converted according to the similar scale. The stacking height of the model soil was 103 cm, the bedrock was 58 cm, the excavation depth of the foundation pit was $H = 40$ cm, and there was a distance B between the station retaining structure and the existing structure. The aspect ratio was $n = B/H$.

According to the requirements of the various mechanical parameters of the model tests, the proportion of the similar material in the model test was determined by conducting several proportioning tests. The mechanical parameters of the raw soils and the similar material are shown in Table 5, and the proportions of the model test similar material is shown in Table 6:

Table 5. Mechanical parameters of the raw soils and the similar material.

Material Type	P (g/cm ³)	E (MPa)	C (kPa)	φ (°)	σ_c (MPa)	Poisson Ratio
Foundation pit soils	2.42	2350	141	24.8	25.5	0.27
Similar materials	2.42	47	2.82	24.8	0.51	0.27

Table 6. Proportion of the similar material in the model test.

$B + I$ /%	B/I	β /%	PA /%	G /%	Mesh no.	S /%
65	7.3	40	6	1.5	40	27.5

Note: B is barite powder; I is iron powder; S is quartz sand; G is gypsum powder; PA is cementing agent; β is the proportion of rosin in cement.

5.2. Model Test Design

According to the size of the foundation pit excavation and the principles of high strength, stability, and easy operation, the test bench was designed; its dimensions were $3\text{ m} \times 1\text{ m} \times 2\text{ m}$. The test bench adopted a frame-type steel frame, which was composed of box-type outer peripheries and a bottom plate for carrying the model soil. High-strength tempered glass was used to simulate the retaining wall, as shown in Figure 8. Stacked hydraulic jacks were used to apply the load uniformly to the model soil through a force transfer device. The excavation project of the metro station foundation pit was simulated by excavating model soil. The model test system consisted of a steel structure bench, data acquisition equipment, and vertical loading hydraulic jacks. The model soil was made using a layered filling method during which similar materials were buried in the test bench to the design height and evenly tamped layer by layer.



Figure 8. Model test bench and model soil backfill.

A uniform distributed load of 14 kN was applied to the adjacent excavation area in order to simulate the initial ground stress field of the soil. The acrylic plate was embedded to simulate the supporting structure, and the earth pressure cells were deployed on the acrylic plate to measure the earth pressure at different layers of the excavation. Figure 9 shows the diagram of the model test. The layout of the monitoring elements and the model soil are shown in Figure 10.

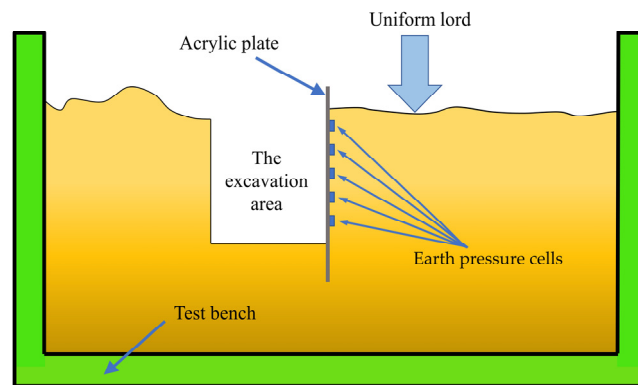


Figure 9. Layout of earth pressure cells and model plate.

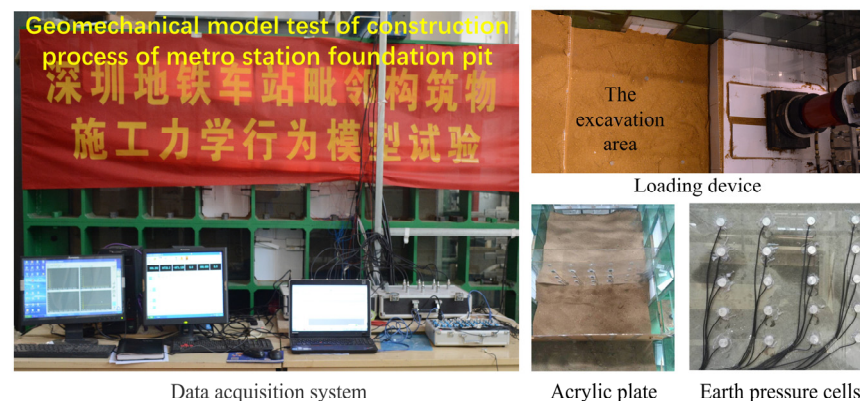


Figure 10. The model test of the metro station excavation.

5.3. Analysis of the Model Test Results

In the model test, working conditions with four different aspect ratios of $n = 0.25$, $n = 0.375$, $n = 0.5$, and $n = 0.75$ were set up. The excavation were divided into four steps. During the test, the changes of earth pressure at each layer were monitored so that the changes of earth pressure under different working conditions in each process were compared and analyzed.

Process 1: the variation curve of the earth pressure against a depth of excavation of 0–10 cm in all working conditions is shown in Figure 11a. The measured values of earth pressure were all less than the calculated value of the Rankine earth pressure theory. The maximum earth pressure occurred under the working condition of $n = 0.50$, which is below the bottom of the excavation and located at a depth of 15 cm.

Process 2: the variation curve of the earth pressure against a depth of excavation of 10–20 cm under all working conditions is shown in Figure 11b. The maximum earth pressure occurred under the working condition of $n = 0.50$, which is below the bottom of the excavation and located at a depth of 15 cm. The excavation process will affect and change the earth pressure of the soil layer below the excavation surface.

Process 3: the variation curve of the earth pressure against a depth of excavation of 20–30 cm under all working condition is shown in Figure 11c. Above the bottom surface of the excavation, the maximum earth pressure occurs under the working condition of $n = 0.50$, which is located at a depth of 15 cm. Below the bottom surface of the excavation, the maximum earth pressure occurred under the working condition of $n = 0.25$, which is located at a depth of 25 cm. The earth pressure at some positions tends to increase.

Process 4: after an excavation of 30–40 cm is completed, the variation curve of earth pressure against depth in all working conditions is shown in Figure 11d. The measured values of earth pressure are all less than the calculated value of the Rankine earth pressure theory in the four working conditions. At 5 cm of excavation, the measured maximum value occurred when $n = 0.75$; at 15 cm of excavation, the measured maximum value

occurred when $n = 0.50$. Before the excavation depth reached 25 cm, the earth pressure had a larger disturbance. Therefore, the corresponding support system should be strengthened during construction in order to prevent excessive earth pressure causing ground failure.

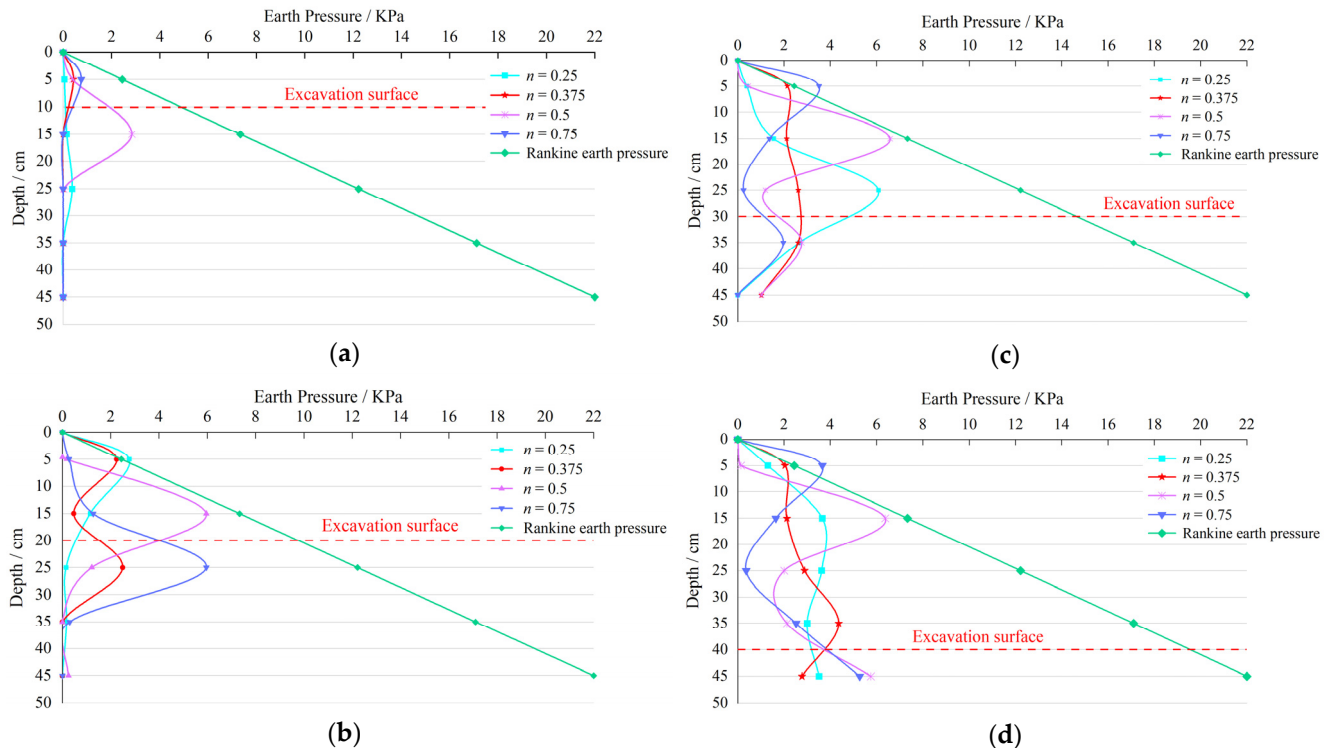


Figure 11. The earth pressure monitored from model test during the excavation process: (a) process 1, (b) process 2, (c) process 3, (d) process 4.

The model test indicates that the similar material ensures accurate and stable mechanical properties during the model excavation, when the mechanical parameters can be adjusted accordingly in large ranges, providing a reference for the construction simulation of similar underground projects. The monitoring and analysis system adopted in this paper can accurately represent the changes of soil mechanics parameters. The development of a new similar material provides assurance for the success of the model test in terms of materials.

6. Conclusions

This research proposes a new similar material for foundation pit excavation model tests. On the basis of the orthogonal tests, the iron ore powder and barite powder content, the cement content, the molar concentration of the cementing agent, and the mesh number of the quartz sand for four controlling factors, set up at four levels, were used to obtain the corresponding mechanical properties of the similar materials. Taking the Shenzhen metro station expansion project as engineering background, a similar model test was carried out in order to investigate the mechanical characteristics of limited-space foundation pit excavation. Based on the experimental results, the following conclusions were obtained:

1. A new similar material composed of iron ore powder, barite powder, quartz sand, liquid paraffin, rosin, gypsum powder, and water was developed. It can adjust the range of mechanical properties with 0.37–5.37 MPa of uniaxial compressive strength, 42.0–279.0 MPa of elastic modulus, and 2.23–2.65 g/cm³ of gravity. The values of the mechanical parameters of the new similar materials are widely distributed, and thus they can effectively reflect the variation of the physical properties of various soils. Rosin and liquid paraffin can be selected as cementing agents in order to easily adjust the mechanical properties of materials.

2. Range analysis was used to investigate the sensitivity of influence of the different factors on the mechanical parameters of the similar material. The study demonstrated that the cement content has a significant impact on similar materials. In the range of 3–9% cement content, the elastic modulus decreases as the cement content increases, while the compressive strength first increases and then decreases. The mesh number of the quartz sand plays a critical role in controlling the density and cohesion of the specimens.
3. Based on the developed new type of similar material, a 3D geomechanical model test on the excavation process of a metro station foundation pit was carried out. The changing mechanical processes of a limited-space soil mass excavation was stimulated truthfully. It was verified that the similar material can meet the test conditions. The variation and distribution of earth pressure in the test results can provide a practical reference for excavation engineering. The comprehensive effects of adjacent structures should be considered in the construction of a station foundation pit. It is necessary to strengthen the support for parts with large earth pressure changes.

Author Contributions: Conceptualization, Z.Z. and Y.G.; investigation, J.C. and Y.C.; writing—original draft preparation, Z.Z.; project administration, X.Z.; funding acquisition, Y.G. All authors have read and agreed to the published version of the manuscript.

Funding: This research was funded by the National Key R&D Program of China (Grant No. 2021YFB2600800), the National Natural Science Foundation of China (Grant No. 51978425), the Natural Science Foundation of Hebei Province (Grant No. E2021210032), and the Hebei Provincial Central Guidance Local Science and Technology Development Project (Grant No. 226Z5405G).

Institutional Review Board Statement: Not applicable.

Informed Consent Statement: Not applicable.

Data Availability Statement: The data presented in this study are available on request from the corresponding author.

Conflicts of Interest: The authors declare no conflict of interest.

References

1. Dou, F.; Li, X.; Xing, H.; Yuan, F.; Ge, W. 3D geological suitability evaluation for urban underground space development—A case study of Qianjiang Newtown in Hangzhou, Eastern China. *Tunn. Undergr. Sp. Tech.* **2021**, *115*, 104052. [[CrossRef](#)]
2. Xie, H.; Zhang, Y.; Chen, Y.; Peng, Q.; Liao, Z.; Zhu, J. A case study of development and utilization of urban underground space in Shenzhen and the Guangdong-Hong Kong-Macao Greater Bay Area. *Tunn. Undergr. Sp. Tech.* **2021**, *107*, 103651. [[CrossRef](#)]
3. Tao, Y. Analysis of Foundation Pit Design of Metro Station in Complex Environment. *Adv. Mater. Sci. Eng.* **2021**, *2021*, 2995380. [[CrossRef](#)]
4. Zhang, G.; Yan, G. In-Flight simulation of the excavation of foundation pit in centrifuge model tests. *Geotech. Test. J.* **2016**, *39*, 59–68. [[CrossRef](#)]
5. Wang, J.; Xiang, H.; Yan, J. Numerical Simulation of Steel Sheet Pile Support Structures in Foundation Pit Excavation. *Int. J. Geomech.* **2019**, *19*, 05019002. [[CrossRef](#)]
6. Bian, X.; Hu, H.; Zhao, C.; Ye, J.; Chen, Y. Protective effect of partition excavations of a large-deep foundation pit on adjacent tunnels in soft soils: A case study. *B. Eng. Geol. Environ.* **2021**, *80*, 5693–5707. [[CrossRef](#)]
7. Wang, W.; Han, Z.; Deng, J.; Zhang, X.; Zhang, Y. Study on soil reinforcement param in deep foundation pit of marshland metro station. *Heliyon* **2019**, *5*, e02836. [[CrossRef](#)]
8. Augarde, C.; Lee, S.; Loukidis, D. Numerical modelling of large deformation problems in geotechnical engineering: A state-of-the-art review. *Soils. Found.* **2021**, *61*, 1718–1735. [[CrossRef](#)]
9. Zhang, J.; Xie, R.; Zhang, H. Mechanical response analysis of the buried pipeline due to adjacent foundation pit excavation. *Tunn. Undergr. Sp. Tech.* **2018**, *78*, 135–145. [[CrossRef](#)]
10. Stead, D.; Eberhardt, E.; Coggan, J. Developments in the characterization of complex rock slope deformation and failure using numerical modelling techniques. *Eng. Geol.* **2006**, *83*, 217–235. [[CrossRef](#)]
11. Zhou, Z.; Chen, S.; Tu, P.; Zhang, H. An analytic study on the deflection of subway tunnel due to adjacent excavation of foundation pit. *J. Mod. Transp.* **2015**, *23*, 287–297. [[CrossRef](#)]
12. Ye, S.; Zhao, Z.; Wang, D. Deformation analysis and safety assessment of existing metro tunnels affected by excavation of a foundation pit. *Undergr. Space* **2020**, *6*, 421–431. [[CrossRef](#)]
13. Wang, J.; Liu, X.; Xiang, J.; Jiang, Y.; Feng, B. Laboratory model tests on water inrush in foundation pit bottom. *Environ. Earth. Sci.* **2016**, *75*, 1072. [[CrossRef](#)]

14. Zhang, Q.; Hu, J.; Wang, J.; He, P.; Hou, L.; Lin, P.; Song, S. Study on the mechanical behavior of a foundation pit retaining structure adjacent to the pile foundation of a subway station. *Environ. Earth Sci.* **2021**, *80*, 704. [[CrossRef](#)]
15. Wang, G.; Chen, W.; Nie, Q.; Chen, J.; Fan, H.; Zhang, C. Impacts of pit excavation on foundation piles in deep silty soil by centrifugal model tests. *Rock. Soil. Mech.* **2019**, *41*, 399.
16. Liu, Q.; Li, S.; Li, L.; Zhao, Y.; Yuan, X. Development of Geomechanical Model Similar Material for Soft Rock Tunnels. *Adv. Mater. Res.* **2011**, *168*, 2249–2253. [[CrossRef](#)]
17. Bai, J.; Wang, M.; Zhang, Q.; Zhu, Z.; Liu, R.; Li, W. Development and application of a new similar material for fluid–solid coupling model test. *Arab. J. Geosci.* **2020**, *13*, 913. [[CrossRef](#)]
18. Zhao, Y.; Cheng, Z.; Gao, Y.; Wu, S.; Chen, C. Review of geomechanical similar-material test systems. *Arab. J. Geosci.* **2020**, *13*, 906. [[CrossRef](#)]
19. Li, Y.; Li, X.; Zhu, W.S.; Zhang, Q. Study on a New Type of Analogue Material for Geotechnical Tests and Its Applications. *Adv. Mater. Res.* **2008**, *33*, 693–698. [[CrossRef](#)]
20. Chen, X.; Mei, Y.; Zhang, X.; Chen, Q. Development of a Rheology Analogical Material for Time-Based Rock Masses. *Adv. Mater. Res.* **2014**, *838*, 967–971. [[CrossRef](#)]
21. Han, B.; Chen, X.; Song, Y.; Li, H. Research on similar material of rock mass. *J. Wuhan Univ. Hydraulic. Electric Eng.* **1997**, *30*, 6–9. (In Chinese)
22. Ma, F.; Li, Z.; Luo, G. NIOS model material and its use in geo-mechanical similarity model test. *J. Hydroelectr. Eng.* **2004**, *23*, 48–51. (In Chinese)
23. Zhu, W.; Li, Y.; Li, S.; Wang, S.; Zhang, Q. Quasi-Three-dimensional physical model tests on a cavern complex under high in-situ stresses. *Int. J. Rock Mech. Min. Sci.* **2011**, *48*, 199–209.
24. Zhu, W.; Zhang, Q.; Zhu, H.; Li, Y.; Yin, J.; Li, S.; Sun, L.; Zhang, L. Large-Scale geomechanical model testing of an underground cavern group in a true three-dimensional (3-D) stress state. *Can. Geotech. J.* **2010**, *47*, 935–946. [[CrossRef](#)]
25. Zhang, Q.; Gao, Q. Geomechanical modeling of the stability of deep tunnel in Dingji coal mine in China. *Geotech. Geol. Eng.* **2019**, *37*, 3313–3327. [[CrossRef](#)]
26. Huang, F.; Zhu, H.; Xu, Q.; Cai, Y.; Zhuang, X. The effect of weak interlayer on the failure pattern of rock mass around tunnel-Scaled model tests and numerical analysis. *Tunn. Undergr. Sp. Tech.* **2013**, *35*, 207–218. [[CrossRef](#)]
27. Shi, X.; Liu, B.; Xiang, Y.; Qi, Y. A Method for Selecting Similar Materials for Rocks in Scaled Physical Modeling Tests. *J. Min. Sci.* **2018**, *54*, 938–948. [[CrossRef](#)]
28. Yang, S.; Chen, M.; Fang, G.; Wang, Y.; Meng, B.; Li, Y.; Jing, H. Physical experiment and numerical modelling of tunnel excavation in slanted upper-soft and lower-hard strata. *Tunn. Undergr. Sp. Tech.* **2018**, *82*, 248–264. [[CrossRef](#)]
29. Xu, Z.; Luo, Y.; Chen, J.; Su, Z.; Zhu, T.; Yuan, J. Mechanical properties and reasonable proportioning of similar materials in physical model test of tunnel lining cracking. *Constr. Build. Mater.* **2021**, *300*, 123960. [[CrossRef](#)]
30. Yang, M.; Yang, Y.; Zhao, B. Study on the Proportion of Conglomerate Similar Materials Based on the Orthogonal Test. *Shock. Vib.* **2021**, *2021*, 6657323. [[CrossRef](#)]
31. Tian, Q.; Zhang, J.; Zhang, Y. Similar simulation experiment of expressway tunnel in karst area. *Constr. Build. Mater.* **2018**, *176*, 1–13. [[CrossRef](#)]
32. Zhou, Y.; Feng, S.; Li, J. Study on the failure mechanism of rock mass around a mined-out area above a highway tunnel—Similarity model test and numerical analysis. *Tunn. Undergr. Sp. Tech.* **2021**, *118*, 104182. [[CrossRef](#)]
33. Li, L.; Shang, C.; Chu, K.; Zhou, Z.; Song, S. Large-Scale geo-mechanical model tests for stability assessment of super-large cross-section tunnel. *Tunn. Undergr. Sp. Tech.* **2021**, *109*, 103756. [[CrossRef](#)]
34. Lu, H.; Zhang, K.; Yi, J.; Wei, A. A study on the optimal selection of similar materials for the physical simulation experiment based on rock mineral components. *Eng. Fail. Anal.* **2022**, *140*, 106607.
35. Lin, P.; Liu, H.; Zhou, W. Experimental study on failure behaviour of deep tunnels under high in-situ stresses. *Tunn. Undergr. Sp. Tech.* **2015**, *46*, 28–45. [[CrossRef](#)]
36. Li, S.; Wang, H.; Zhang, Q.; Li, Y. New type geo-mechanical similar material experiments research and its application. *Key Eng. Mater.* **2006**, *326*, 1801–1804. [[CrossRef](#)]